**Modeling the Sequestration of $CO_2$ in Deep Geological Formations**

K. Prasad Saripalli, B. Peter McGrail, and Mark D. White
Pacific Northwest National Laboratory, Richland, Washington 99352

corresponding author

Prasad Saripalli
Senior Research Scientist
Pacific Northwest National Laboratory
1313 Sigma V Complex (K6-81)
Richland, WA 99352
ph: (509) 376-1667
fax: (509) 376-5368
prasad.saripalli@pnl.gov

**Modeling the Sequestration of $CO_2$ in Deep Geological Formations**

K. Prasad Saripalli, B. Peter McGrail, and Mark D. White
Pacific Northwest National Laboratory, Richland, Washington 99352

Modeling the injection of $CO_2$ and its sequestration will require simulations of a multi-well injection system in a large reservoir field. However, modeling at the injection well scale is a necessary prerequisite to reservoir scale modeling. We report on the development and application of two models: 1) a semi-analytical model (PNLCARB), and 2) a numerical model (STOMP-$CO_2$). PNLCARB can simulate multiphase, radial injection of $CO_2$ and the growth of its area of review around the injector, buoyancy-driven migration of $CO_2$ toward the top confining layer, and dissolution of $CO_2$ during injection and vertical migration. Phase behavior algorithms for the physicochemical properties $CO_2$, including the supercritical region, were also added to the Subsurface Transport Over Multiple Phases (STOMP) simulator. The models effectively simulate deep-well injection of water-immiscible, gaseous, or supercritical $CO_2$. The effect of pertinent fluid, reservoir, and operational characteristics on the deep-well injection of $CO_2$ was investigated. Results indicate that the injected $CO_2$ phase initially grows as a bubble radially outward, dissolves partially in the formation waters, and eventually floats toward the top confining layer due to buoyancy effects. Formation permeability, porosity, injection rate and pressure, and dissolution of $CO_2$ influence the growth and ultimate distribution of the $CO_2$ phase.

***Key Words***

Carbon sequestration, underground $CO_2$ storage, deep-well injection, modeling

***Introduction***

Geological sequestration of $CO_2$ has been recognized as an important strategy for reducing the $CO_2$ concentration in the atmosphere. Our research in this area is focused on developing economically viable technologies for geological sequestration and models describing the same. Following is a brief description of 1) a semi-analytical model (PNLCARB), and 2) a numerical model (STOMP-CO2), for the simulation of deepwell injection of $CO_2$.

The primary processes affecting the injection and geological sequestration of $CO_2$ are: (i) multiphase, radial injection of $CO_2$ and the growth of the $CO_2$ bubble around the injector, (ii) buoyancy-driven migration of $CO_2$ toward the top aquifer confining layer, (iii) escape of $CO_2$ through leakage (iv) dissolution of $CO_2$ during injection and vertical migration,

and the resulting aqueous speciation of carbon, (v) carbon mass exchange via precipitation and dissolution of minerals through the interaction of dissolved and gaseous phase $CO_2$ with the formation, (vi) changes in hydrogeological properties due to mineral trapping and the resulting formation damage, injectivity decline and fracturing.

Weir *et al.* [3] presented a numerical modeling study of $CO_2$ injection and sequestration using the reservoir code TOUGH2, without considering the dissolution of $CO_2$ and its escape through leaks. Lindeberg [4] used the Eclipse 100 reservoir simulator to model the escape of $CO_2$ from aquifers. Law and Bachu [5] used a two-dimensional numerical model to assess the hydrodynamic trapping capacity of two aquifers in Canada. Recently, McPherson and Cole [6] also used the TOUGH2 reservoir simulator to model the sequestration of $CO_2$ in the Powder River Basin, Wyoming. Often, single well radial injection/extraction models are able to model many important physico-chemical phenomena around a single well in a more detailed fashion than the typical numerical models, which are better suited for modeling at a larger scale (*e.g.,* a multiple well reservoir field).Several researchers have shown earlier that analytical and semi-analytical models of radial injection are valuable and easy-to-use tools for modeling diverse injection well operations, such as gas injection [7, 8], gas hydrate production [9], produced water reinjection [10,11], well stimulation [12] and hazardous liquid waste injection [13].

**PNLCARB: A Semi-analytical Modeling Framework**

Simple and easy-to-use modeling tools would be valuable in assessing the performance of sequestration during and after injection. PNLCARB (Saripalli and McGrail, 2001; [26]) is a semi-analytical model to simulate the deep-well injection of $CO_2$ for geological sequestration. The model is based on equations governing the radial injection of an immiscible $CO_2$ phase into saturated confined formations representing deep saline aquifers and reservoirs. It can simulate axisymmetric flow around the injector, including buoyancy-driven flow with simultaneous dissolution of $CO_2$. The effect of pertinent fluid, reservoir and operational characteristics on the deep-well injection of $CO_2$ can be

investigated. The model may be extended to include phenomena affecting sequestration and injection, such as mineral trapping, formation damage, well injectivity, stimulation and fracturing [11, 12].

We limit the scope of the model to confined, porous formations bearing water/brine with radial injection at a constant rate under isothermal conditions. At typical reservoir temperatures and pressures (*e.g.,* 70 $^{o}$F, 3000 psi), the phase behavioral properties such as density of $CO_2$ vary only moderately with temperature [2], as will be shown later in the phase behavior calculations. As such, assuming isothermal injection is reasonable. The first three of the processes described above are mainly flow-related, driven by inertial forces whereas the later three involve chemical reactions. Development of a semi-analytical model integrating the effects of these phenomena is outlined in the following sections. A more detailed on the development of this model can be found elsewhere (Saripalli and McGrail, 2001).

***(i) Radial injection of supercritical $CO_2$ fluid***

Deep-well injection of $CO_2$ is a multiphase flow phenomenon, where a slightly compressible supercritical fluid drives water radially outward, and also migrates upward due to buoyancy. Injection of gases into gas storage reservoirs was modeled earlier as single phase radial encroachment [8, 14]. Recently, steady state injection of $CO_2$ as a supercritical fluid was modeled using Darcy's law [3,4] for the flow of two immiscible phases. It should be noted that the injection and radial migration of immiscible $CO_2$ phase into an initially water saturated formation involves simultaneous flow of $CO_2$ and water. For an incompressible $CO_2$ phase, the equations governing the simultaneous flow of $CO_2$ and water can be written as:

$$\nabla \cdot v_{r,i} + \phi \frac{\partial S_i}{\partial t} = 0 \qquad (1)$$

for both water ($i = w$) and $CO_2$ ($i = c$) phases. In Eq. 1, $S_i$ is saturation of phase $i$, $\phi$ is porosity and $v_{r,i}$ is the radial velocity of phase $i$, given as:

$$v_{r,i} = \frac{Q_i f_i(S_i)}{2\pi r h} \qquad (2)$$

where $f_i$ is the fractional flow of phase $i$, injected at a constant rate of $Q_i$. Upon substitution of (2) into (1), the radial flow equation for the immiscible injected phase becomes [7]:

$$\frac{Q_c f_c}{2\pi r h \phi}\frac{\partial S_c}{\partial r}+\frac{\partial S_c}{\partial t}=0 \qquad (3)$$

which is based on the Buckley-Leverette two phase displacement theory. Buckley-Leverette theory predicts that the saturation of the injected phase decreases away from the injection well. Woods and Comer [7] solved Eq. 3 for the radial injection of gases into a gas storage reservoir initially saturated with water with the boundary condition that $r=r_w$ at $t=0$, and obtained the following analytical solution:

$$r_s=\left(\frac{f_c^{'}}{\pi h\phi}Q_c t+r_w^2\right)^{1/2} \qquad (4)$$

where $r_s$ is the radius of a gas-rich zone around the injector, with its outer periphery corresponding to a gas saturation of $S_g$.

Fractional flow of the $CO_2$ phase, $f_c$, and its derivative $f_c^{'} = df/dS_c$, required for the determination of $CO_2$ bubble front ($r_s$) via Eq. 4, are calculated using an extension of the Brooks-Corey relative permeability relationships [15]. At any time $t$, the radius of the cylindrical two-phase zone containing a $CO_2$ saturation of $S_{c,o}$ at its periphery is obtained by substituting $df/dS_c$ into Eq. 4. The $CO_2$ saturation within such radial zone varies as a non-linear function of the radial distance away from the well, with high $S_c$ values near the well-bore and increasingly lower $S_c$ values toward the periphery. Using Eq. 4 as a basis, $r_s$ vs. $t$ and $S_c$ vs. $r$ profiles, which together describe the growth and morphology of the injected $CO_2$ bubble, can be obtained during injection. These profiles are useful for obtaining the volumes of free-phase and dissolved $CO_2$ at any time.

The average $CO_2$ saturation at any time $t$, within a cylindrical bubble domain of radius $r_s$ and formation thickness $h$ is given as:

$$\overline{S}_c=\frac{1}{\pi r^2\phi h}\int_{r=0}^{r=r_s}2\pi r\phi h S_c dr \qquad (5)$$

It will be shown (Fig. 1) that the typical $S_c$ vs. $r$ relationship obtained using the above procedure follows a rapid decrease in $S_c$ with $r$, and can be modeled, for the purpose of integration and the calculation of $\overline{S}_c$ using Eq. 5, by an empirical equation fit of the form:

$$S_c = m \ln r + n \tag{6}$$

where $m$ and $n$ are constants. Upon substitution of Eq. 6 in Eq. 5 and integration, one obtains the average $CO_2$ saturation in a cylindrical zone of radius $r_s$, with the saturation on its periphery of $S_{c,o}$.

It was shown earlier [16,17] that the phase partitioning behavior of $CO_2$-$H_2O$ mixtures can be described using various equations of state. We use the P-V relationship for $CO_2$ based on the Plank and Kuprianoff equation of state [17] given below, which was shown to be in good agreement with experimental data for $CO_2$:

$$V = \frac{RT}{P} - \left( \frac{0.0825 + 1.225^{-07} P}{\left( \frac{T}{100} \right)^{10/3}} \right) \tag{7}$$

This P-V relationship is fairly insensitive to temperature, in the temperature range of interest during injection and sequestration (32 to 125 $^{o}$F). Further, analysis of carefully measured solubility data [18] revealed that, in the range of pressures typically experienced during injection (1000 to 4000 psi), the pressure dependence of $CO_2$ solubility can be adequately described using a linear model. Salinity of the reservoir water does not significantly influence the solubility of CO2 (< 10% reduction in solubility as salinity increases from 0 to 25 parts per thousand)[19]. The effect of salinity on $CO_2$ dissolution is not considered in the present model. Assuming instantaneous equilibrium, we model the dissolution of the injected $CO_2$ into resident water phase as:

$$C_w = K_1 - K_2 P(r) \tag{8}$$

The linear dissolution model is suitable within the ranges of pressures (1000-3000 psi) and temperatures (32 to 120 $^{o}$F) chosen in this study.

It should be noted that both $S_c$ and $P(r)$ are non-linear functions of $r$. Knowledge of the pressure distribution is crucial for an accurate assessment of the dissolved phase

concentration which varies with pressure according to Eq. 8. Similarly, the pressure distribution play a vital role in the modeling of the injectivity decline due to mineral or particle trapping and initiation and growth of fractures around injection wells [11, 20]. The pressure distribution in the radial two-phase flow region at radius $r$ is given as [7]:

$$P(r) = \frac{Q}{2\pi hk} \int_{r_w}^{r_s} \frac{dr/r}{\left[ \frac{k_{rc}(r)}{\mu_g} + \frac{k_{rw}(r)}{\mu_w} \right]} \tag{9}$$

Relative permeabilities in Eq. 9 vary with $r$, since $CO_2$ and water saturations vary with $r$ (Eq. 4). Upon integration, Eq. 9 yields the pressure distribution in the $CO_2$ phase around the injector. A knowledge of the pressure distribution in the $CO_2$ phase around the injection well is essential for modeling of critical injection-related phenomena such as well stimulation [12] and fracturing [20, 21].

The volume of $CO_2$ dissolved in the aqueous phase in a volume element of radial length $dr$, at any bubble radius $r$ is taken as

$$dV_d = 2\pi r C_w \phi \left( h_b (1 - S_c) + (H - h_b) \right) dr \tag{10}$$

where $H$ is the thickness of the host formation and $h_b$ is the thickness of the floating $CO_2$ bubble at radial distance $r$. The first and second terms within the parenthesis on the right hand side of Eq. 10 represent respectively the volume of $CO_2$ in dissolved in water below and above the $CO_2$-water contact. Integrating Eq. 10 between limits $r = r_w$ to $r_s$ yields the total dissolved phase volume of $CO_2$ at any time $t$. Free phase volume of $CO_2$ is then the difference between the injected and dissolved volumes:

$$V_f = V_{inj} - V_d \tag{11}$$

Eq. 11 is predicated upon the assumption that the reservoir rock is truly water wet, and hence has no direct contact with the free phase $CO_2$. Mineral trapping of $CO_2$, which may occur due to the dissolved phase $CO_2$ contacting the rock mineral surfaces, is not considered in the present model. Eq. 1 through 11 represent some of the basic equations that govern the radial growth and dissolution of $CO_2$ bubble and the pressure and saturation distributions of $CO_2$ within this bubble region.

***Buoyancy Driven Floating of $CO_2$ bubble:***

Due to the density difference between reservoir water and $CO_2$, the $CO_2$ bubble will eventually float toward the top confining layer, and water will gravitate to the bottom layers. However, only a fraction of the total injected volume of $CO_2$ will be available to float toward the top, as the remaining volume is dissolved in the resident water phase. Strictly speaking, the phenomena of $CO_2$ dissolution and buoyant floating need to be coupled, to model their combined effect on the final distribution of $CO_2$ realistically. However, the velocity with which the buoyant floating of $CO_2$ occurs at any radius $r$ is given as:

$$v_h = -\frac{Kk_{r,c}}{\mu}\Delta\rho g \tag{12}$$

At typical rates and pressures of injection, the radial velocity in the near-field, where most of the injected $CO_2$ resides, is several times larger than the vertical velocity component. As such, modeling the buoyant floating of $CO_2$ within the area of review over longer periods of time may be decoupled from radial injection. We model the dissolution of free-phase $CO_2$ in the formation water as an instantaneous, equilibrium dissolution process. This is accomplished at any location ($r$, $t$) by solving Eq. 15 using the corresponding $S_c$ value. The local dissolved phase volume ($dV_d$) in individual volume elements located at a radial distance $r$ from the injector are obtained directly from Eq. 15, without integration. The resulting $dV_d$ is used to calculate the final free phase $CO_2$ volume ($dV_f$) at a given radius $r$, using a differential form of Eq. 11. This free phase volume is assumed to float toward the top of the formation (near the cap rock). The resulting bubble profile floating near the 'roof' of the confined formation will have the maximum $S_c$ closer to the injection well and minimum $S_c$ away from it, following the same $S_c$-$r$ distribution represented by Eq. 4 (Fig. 1). Assuming no further dissolution in the $CO_2$ saturated water, a part of this free phase $CO_2$ floating near the roof can be lost to the atmosphere due to leaking.

***Leaking of $CO_2$ to Atmosphere***

Escape of $CO_2$ due to leakage through the confining layers is a concern, because leakage of $CO_2$ in large quantities would compromise safety as well as the objectives of

sequestration. Three pathways that could mediate the leakage of $CO_2$ to the atmosphere are (i) vertical migration as a free phase through fractures, (ii) buoyancy driven flow through permeable zones of a water saturated cap rock, and (iii) diffusion as a dissolved phase through a water saturated cap rock. Among these processes, (i) and (ii) are likely to be more significant. For free phase $CO_2$ to enter a pore or fracture of size $2d$, the capillary pressure ($P_c$) needs to be $\geq 2\sigma/d$, where $\sigma$ is the $CO_2$-brine interfacial tension. The vertical buoyant pressure exerted on the top confining layer by the $CO_2$ bubble floating at the top is:

$$P_b = \Delta\rho g h_b \tag{13}$$

where $\Delta\rho$ is the density difference between the brine and $CO_2$ and $h_b$ is the thickness of the $CO_2$ bubble floating near the top confined layer. For $CO_2$ to enter the cap rock through the fracture, $P_b$ must exceed $P_c$, thus satisfying the following condition:

$$h_b \geq \frac{2\sigma}{\Delta\rho g d} \tag{14}$$

Rate of flow of free phase $CO_2$ through a vertical fracture of aperture $2d$ , length $l_f$ and width $w$ is given as:

$$q_f = \frac{\Delta\rho g w d^3}{12\mu}\left(\frac{dH_c}{dz}\right) \tag{15}$$

where $H_c$ is the $CO_2$ head causing flow along the vertical direction ($z$). In the case of a continuous fracture connecting the confined formation to the ground surface, the gradient term in Eq. 20 is equal to $h_c/(h_c+l_f)$.

**Results and Discussion**

Simulations were conducted using a fully-screened, perforated injection well, injecting $CO_2$ into a 160 m thick sandstone formation bounded by impermeable layers at the top and bottom. The injection and formation parameters for the base case, chosen to represent a typical deep-well gas injection operation, similar to the base case simulation of Lindberg [4], are summarized in Table 1. Injection well is assumed to be fully screened over the thickness of the formation.

Table 1. Base Case Injection and Formation Parameters

| | |
|---|---|
| Well radius = 15 cm | Formation permeability = 1 Darcy |
| Drainage radius = 1540 m | Formation thickness = 160 m |
| Injection rate (constant) = 27397 cum/day | Viscosity of $CO_2$ phase, $\mu_g$ = 0.000043 Pa.s |
| Injection Pressure, $P_w$ = 2545.5 psi | Viscosity of water, $\mu_w$ = 0.00043 Pa.S |
| Far-field boundary pressure, $P_e$ = 2500 psi | |

Shown in Fig. 1 is the distribution of injected $CO_2$ saturation at 10000 days after the commencement of injection. The $CO_2$ saturation is the highest near the injector, decreasing radially outward. According to the Buckley-Leverette model, the leaky piston type displacement of resident water by injected $CO_2$ results in such saturation distribution [7]. Shown in Fig. 2 are the radii of a zone around the injector whose outer periphery has a $CO_2$ saturation of $S_o$, for different values of $S_o$, demonstrating the growth of the $CO_2$ bubble as a function of time after commencing injection. The predictions agree with the results of Lindberg [4], who used a numerical model Eclipse 100, to simulate the same base case shown in Table 1, indicating that semi-analytical approaches are useful for a rapid prediction and assessment of deep-well injection of $CO_2$. Shown in Fig. 3 is the pressure distribution in the injected $CO_2$ phase, as a function of distance from the well.

The $CO_2$ bubble growing during injection simultaneously dissolves in the formation waters and migrates upwards due to buoyancy. As a result, the $CO_2$ bubble recedes radially inwards, and floats toward the top confining layers. Shown in Fig. 4 are results from a set of simulations where $CO_2$ was injected for a period of 10,000 days, and then allowed to dissolve and float. The curves represent the shape of the immiscible $CO_2$–water contact for two different injection rates, after the completion of buoyant floating and equilibrium dissolution, and the region above this contact rich in free-phase $CO_2$, distributed radially (as shown in Fig. 1). As can be seen from Fig. 4, the injected $CO_2$ phase receded radially and floated vertically upward, after a part of it being dissolved in the formation water. In the long term, a part of this dissolved carbon may be permanently sequestered as a mineral phase[5], the remaining mass being redistributed by dilution among the formation waters via advection and diffusion. The thin free phase $CO_2$ layer

floating at the top will serve as a source for diffusive flux into the formation waters as well as escape into the atmosphere and/or overlying aquifer via fractures and high permeability conductive zones within the top cap rock.

***Leakage Calculations:*** Assuming a density difference of 400 kg/m$^3$ between brine and $CO_2$ and a bubble thickness $h_b$ m, the buoyant pressure exerted on the cap rock will be 3924 $h_b$ Pa. Assuming a $CO_2$-brine interfacial tension of 35 mN/m, it requires an entry pressure of 0.07/$d$ Pa for the $CO_2$ to break into the water saturated cap rock. Thus, for $CO_2$ to enter the cap rock, the minimum floating bubble's thickness ($h_b$) should be 17.83 m. It can be seen from Fig. 4 that the floating bubble thickness is 20 m or larger near the injection well for the base case simulation. Therefore, if microcracks or crevices of width of at least 2 microns are available in the cap rock's structure, a $CO_2$ bubble thickness of 17.83 m would be sufficient to cause leakage. The rate of flow of such leakage is calculated to be 23.52 m$^3$/year, using Eq. 20. For a fracture 10 m wide and half-aperture on the order of a millimeter, in contact with the free-phase $CO_2$ bubble 20 m thick on one end and passing through an over-burden 20 m thick to the atmosphere, the volumetric leakage rate would be 2.35 x $10^6$ m$^3$/year, approximately 1% of the total volume of injected during the 10,000 day injection of the base case. Clearly, leakage of free-phase $CO_2$ can be a significant pathway for the loss of sequestered $CO_2$, if cracks and crevices are present through the overburden.

**Limitations**

While the model presented here can simulate the basic features of a typical $CO_2$ deep-well injection operation, it is based on the assumption of uniform formation properties, constant rate of injection and instantaneous dissolution of $CO_2$. Allowing for variable injection pressures and heterogeneous formation properties will be necessary to adequately model field operations. Due to the low Reynold's number (laminar flow) environment in a typical waste reservoir, dissolution of $CO_2$ is likely to be a rate limited process, governed by the morphology of the $CO_2$-water contact, $CO_2$ phase pressure, temperature and the water composition. A rate-limited dissolution model using a variable $CO_2$ dissolution rate may be necessary to simulate the dissolution non-equilibrium

adequately. Further, fluid injection wells often lose their initial injectivity due to the plugging of formation around the injector by particles, oil droplets and precipitates [10]. Based on the geochemistry of $CO_2$-rock interactions in carbonate and sandstone reservoirs, such formation damage and injectivity decline may be expected [24] during the deep-well injection of fluid $CO_2$ into deep geological formations. The effect of mineral trapping of $CO_2$ on injectivity decline should be included in models simulating deep-well injection. Apart from such limitations, analytical approaches to the modeling of deep-well injection were shown to agree with field data earlier [7, 24]. The basic modeling framework presented allows the integration of such additional features.

**STOMP-CO2: A Numerical Multiphase Flow and Transport Simulator**

Advanced computational tools are available at PNNL to conduct modeling studies of the $CO_2$ injection process. Fully coupled fluid, heat, and mass transport modified by kinetic and/or equilibrium controlled chemical reactions can be modeled using PNNL's STOMP-$CO_2$ and STORM simulators. Temporal and spatial responses to the injection of $CO_2$ can be simulated using STORM, including heat transfer associated with injection, if necessary. Changes in transport properties of the gases and fluids in the reservoir, and well injectivity can be evaluated by monitoring the formation of $CO_2$ mineral precipitates and computing its impact on porosity and permeability.

Injection of $CO_2$ can lead to changes in hydraulic properties of the sediments. Without careful control of the injection-production process, solid (e.g., mineral) trapping could lead to formation damage and well blow out [10] with concomitant poor utilization of reservoir capacity for $CO_2$ sequestration. Hydrogeologic properties, especially the porosity and relative permeabilities to $CO_2$ and water will change with time during the injection process. Experimental measurement of these changes is necessary to adequately model the process. STORM can be used, with the experimental data in tandem, to examine the dynamics of the coupled multiphase flow and reactive transport steps that accompany the $CO_2$ Injection process and its impact on formation damage.

Phase behavior algorithms for the physicochemical properties $CO_2$, including the supercritical region were added to the Subsurface Transport Over Multiple Phases (STOMP) simulator [26]. The model effectively simulates deep-well injection of water-immiscible, gaseous, or supercritical $CO_2$. Shown in Fig. 5 are the CO2 bubble growth profiles from a base case simulation using STOMP-CO2.

**Conclusions**

Equations governing the radial injection of an immiscible $CO_2$ phase into confined formations (representing deep saline aquifers and reservoirs), its axisymmetric flow around the injector and eventual buoyancy-driven transport with simultaneous dissolution and were developed. It was shown that formulation based on Buckley-Leverette theory treating the process as a simultaneous multiphase injection adequately describes the injection and migration of $CO_2$ around the well. The effect of pertinent fluid, reservoir and operational characteristics on the deep-well injection of $CO_2$, bubble growth and dissolution was investigated. The results indicate that the injected $CO_2$ initially grows as a bubble radially outward. This bubble eventually dissolves in the formation waters, floats toward the top due to buoyancy and settles near the top confining layer. An increase in injection rate was found to increase the dimensions of bubble and hence the total volume of $CO_2$ sequestered. A decrease in the formation porosity resulted in a corresponding increase in the radius of the $CO_2$ bubble; this does not necessarily mean an increase in the total mass of $CO_2$ sequestered, because lower porosity implies a lower formation pore volume.

**References**

1. Herzog, H. J., Drake, E. M., Adams E. E.: $CO_2$ capture, reuse and storage technologies for mitigating global climate change. Final report, DOE No. DE-AF22-96PC01257, MIT, Cambridge, MA, 1977.

2. Bachu, S.: Sequestration of $CO_2$ in geological media: criteria and approach for site selection in response to climate change, *Energy Convers. Mgmt.* Vol. 41, pp. 953-970, 2000.

3. Weir, G. J., White, S. P. and Kissling, W. M.: Reservoir Storage and Containment of Greenhouse Gases, *Energy Convers. Mgmt.* Vol. 36, No. 6-9, pp. 531-534, 1995.

4. Lindeberg, E.: Escape of CO2 from Aquifers, *Energy Convers. Mgmt.* Vol. 38, pp. 235-240, 1997.

5. Law, D. H.-S. and Bachu, S.: Hydrogeological and numerical analysis of $CO_2$ disposal in deep aquifers in the Alberta sedimentary basin, *Energy Convers. Mgmt.* Vol. 37, pp. 1167-1174, 1996.

6. McPherson, B.J.O.L and Cole, B. S. : Multiphase $CO_2$ flow, transport and sequestration in the Powder River basin, Wyoming, USA, *J. Geochem. Explo*., pp. 65-69, Vol. 69-70, 2000.

7. Woods, E. G. and Comer, A. G.: Saturation distribution and injection pressure for a radial gas-storage reservoir, *J. Petroleum Tech*., pp.1389-1393, 1962;

8. Katz, D. L. and Coats, K. H. : *Underground storage of fluids*, Ulrich's books Inc., Ann Arbor, MI, 1968.

9. Selim, M. S. and Sloan, E. D.: Hydrate Dissociation in Sediment, *SPERE* (May 1990), pp. 245-51.

10. Saripalli, K. P., Sharma, M. M. and Bryant, S. L.: Modeling the injection well performance during deep-well injection of liquid wastes", *J. Hydrology,* Vol. 227, 41-55, 2000.

11. Saripalli, K. P., Gadde, B., Bryant, S. L. and Sharma, M. M.: Modeling the Role of Fracture Face and Formation Plugging in Injection Well Fracturing and Injectivity Decline, SPE Paper# 52731 presented at *the SPE/EPA Exploration and Production Conference*, Austin, TX, 1999.

12. Schechter, R. S. (1992) "*Oil Well Stimulation*" Prentice Hall, Englewood Cliffs, NJ., pp. 203-207.

13. Kuo, C. H.: Pressure behavior in subsurface disposal of liquid industrial wastes, *WPCF Journal,* Vol. 44 (12), pp. 2325-3, 1972.

14. Jenkins, R. and Aronofsky, J. S.: Unsteady radial flow of gas through porous media, *J. Apl. Mech., ASME*, Vol. 20, pp. 210-214, 1953;

15. Corey, A. T. *Mechanics of Immiscible Fluids in Porous Media*, Water Resources Publications, Highlands Ranch, CO, 1994.

16. Shyu, C., Hanif, N. S. M., Hall, K. R. and Eubank, P. T.: Carbon dioxide-water phase equilibria results from the Wong-Sandler combining rules, *Fluid Phase Equilib.* Vol. 130, pp. 73-85, 1997.

17. Quinn, E. L. and Jones, C. L.: Carbon Dioxide, *Am Chem. Soc. Monograph*, Reinhold Publishing Corporation, New York, NY, 1936.

18. Wiebe, R. and Gaddy, V. L.: The solubility in water of carbon dioxide at 50, 75 and 100 $^{o}$C at pressures to 700 atmospheres*, J. Am. Chem. Soc.*, 61: 315, 1939.

19. Colt, J.: Computation of dissolved gas concentrations in water as functions of temperature, salinity and pressure, *American Fisheries Society Special Publication No.* 14, AFS, Bethesda, MD, pp. 55, 1984.

20. Bryant, S. and Saripalli, K. P.: Flow and Contaminant Transport around a Single, Growing Fracture, submitted to *Adv. Water Resources*, 2000.

21. Perkins, T. K. and Gonzalez, J. A. "The Effect of Thermoelastic Stresses on Injection Well Fracturing," *SPE Journal*, February 1985, 78-88.

22. Lindberg, E. and Wessel-Berg, D.: Vertical convection in an aquifer column under a CO2 gas cap, *Energy Convers. Mgmt.* Vol. 38, suppl., pp. 229-234, 1997.

23. Sayegh, S. G., Krause, F. F., Girard, M. and DeBree, C.: Rock/fluid interactions of carbonated brines in a sandstone reservoir: Pembina Cardium, Alberta, Canada, SPE Paper#19392, *SPE Form. Eval*., pp. 399-405, 1990.

24. Pang, S. and M.M. Sharma: A Model for Predicting Injectivity Decline in Eater Injection Wells" Paper SPE28489 presented at the *SPE 69th Annual Technical Conference and Exhibition* in New Orleans, 25-28 Sep. 1994, pp. 275-284.

25. White, M.D., and M. Oostrom, STOMP: Subsurface Transport Over Multiple Phases, Theory Guide, Pacific Northwest National Laboratory, Richland, Washington, 1996.

26. Saripalli, K. P. and McGrail, B. P (2001). "Modeling Deep-well Injection of $CO_2$ for Geological Sequestration" (in press) *Energy Conversion & Management.*

**Nomenclature**

$C_w$ = concentration of $CO_2$ in water as a volume fraction
$d$ = half-aperture size of fracture (L)
$f_i$ = fractional flow to phase $i$
$g$ = acceleration due to gravity ($LT^{-2}$)
$H$ = formation thickness (L)
$H_c$ = $CO_2$ head causing flow through a fracture (L)
$h_b$ = thickness of $CO_2$ bubble floating at the top (L)
$K$ = formation permeability ($L^{-2}$)
$k_{r,i}$ = relative permeability to phase $i$
$l_f$ = length of the fracture (L)
$m$ = an empirical constant

$n$ = an empirical constant
$\Delta P$ = pressure drop ($ML^{-1}T^{-2}$)
$Q_i$ = volumetric flow rate of phase $i$ ($L^3/T$)
$r$ = radial distance, measured from well center (L)
$r_w$ = well radius (L)
$r_s$ = radius of $CO_2$ zone corresponding to a $CO_2$ saturation $S_g$ (L)
$r_{in}$ = drainage radius (L)
$S_c$ = saturation of $CO_2$
$t$ = time (T)
$V_{inj}$ = injected volume of $CO_2$ ($L^3$)
$V_o$ = volume of formation occupied by $CO_2$ ($L^3$)
$V_d$ = dissolved phase volume ($L^3$)
$v_{r,i}$ = superficial (Darcy) radial velocity for phase $i$ (L/T)
$v_h$ = vertical component of velocity (L/T)
$w$ = width of the fracture (L)
$\phi$ = formation porosity
$\lambda$ = Brooks-Corey parameter
$\mu_i$ = viscosity of phase $i$ ($ML^{-1}T^{-1}$)
$\sigma$ = interfacial tension ($MT^{-2}$)
$\rho$ = density ($ML^{-3}$)

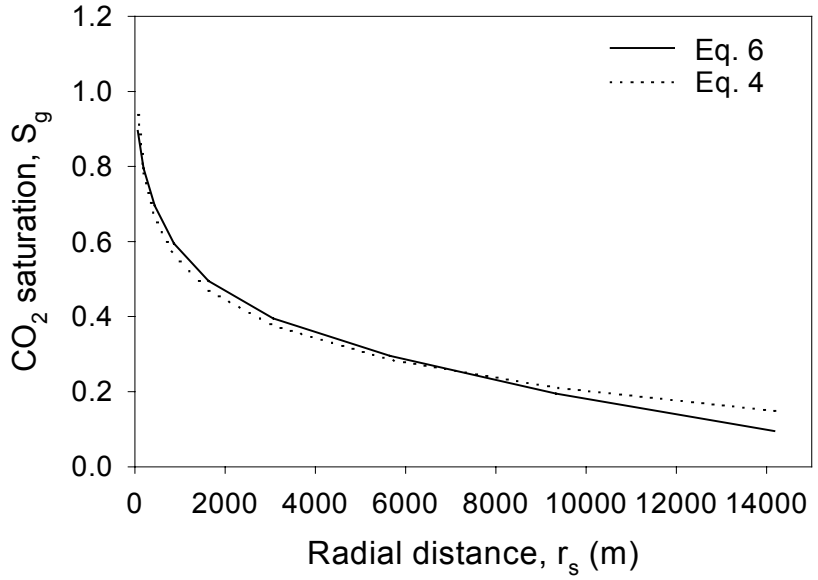


Fig. 1. CO2 saturation distribution after 10000 days of injection as predicted by Buckley-Leverett theory (Eq. 4) and an empirical model fit (Eq. 8), using m = -0.148 and n = 1.5634 (R2 = 0.983)

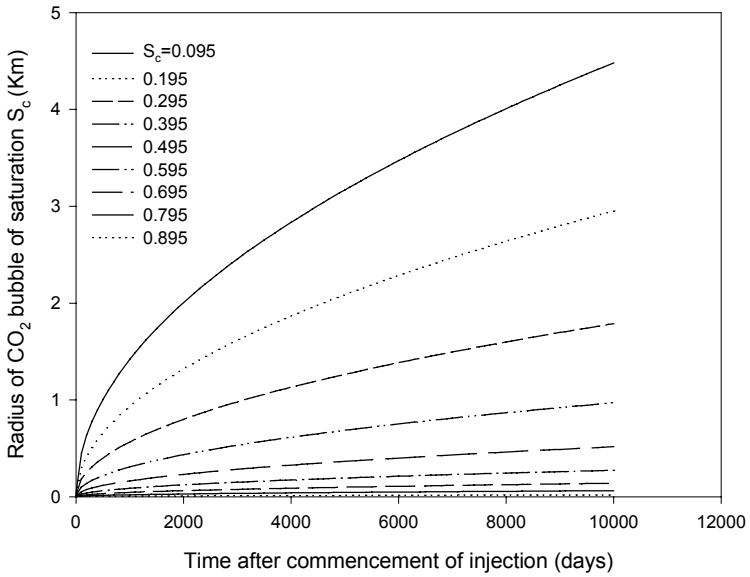


Fig. 2. Radius of the $CO_2$ bubble corresponding to a saturation $S_c$ (given in legend) after 10000 days of injection.

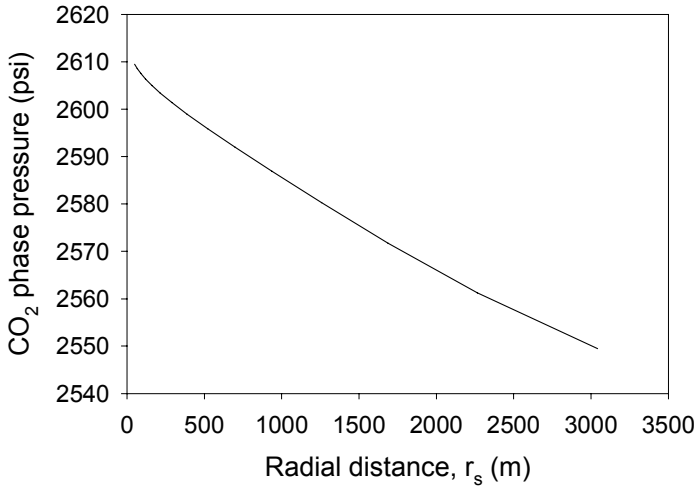


Fig. 3. $CO_2$ phase pressure distribution after 10000 days of injection.

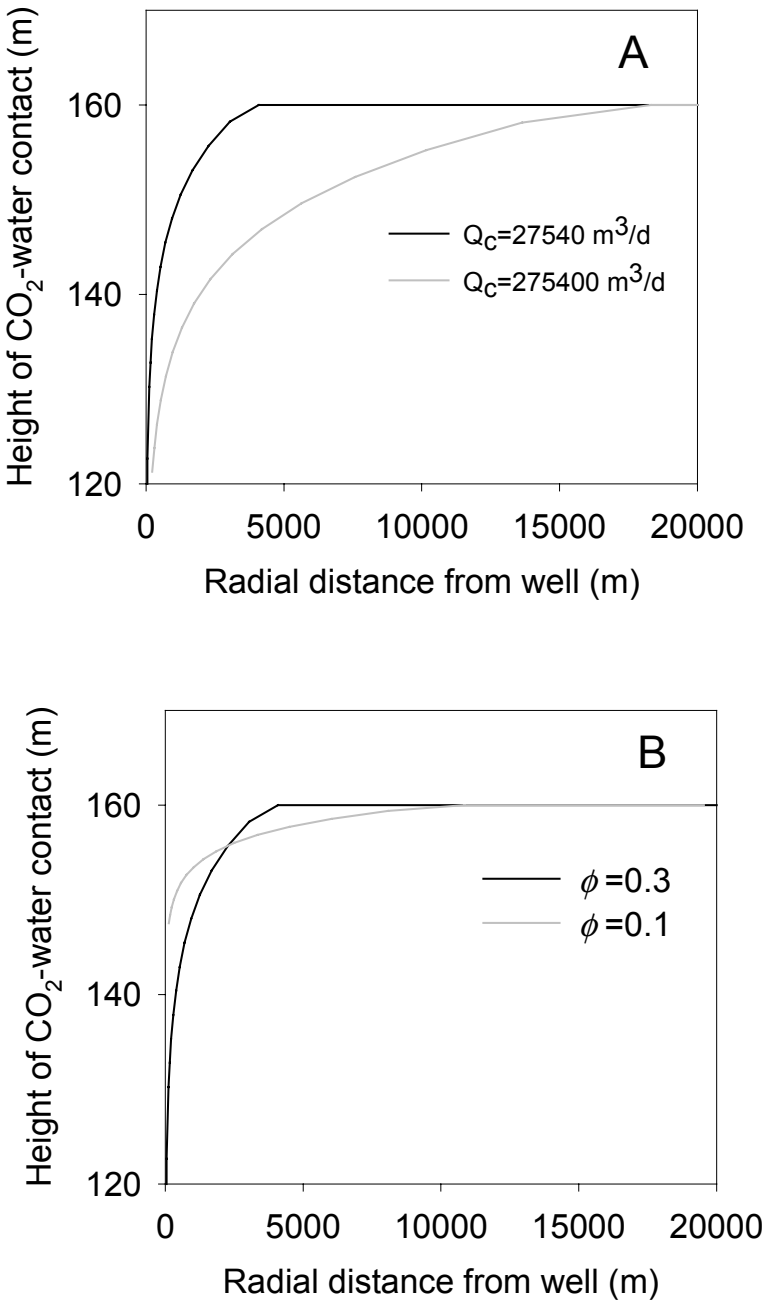


Fig. 4. Effect of (a) injection rate (b) porosity and on the final distribution of free-phase $CO_2$ bubble

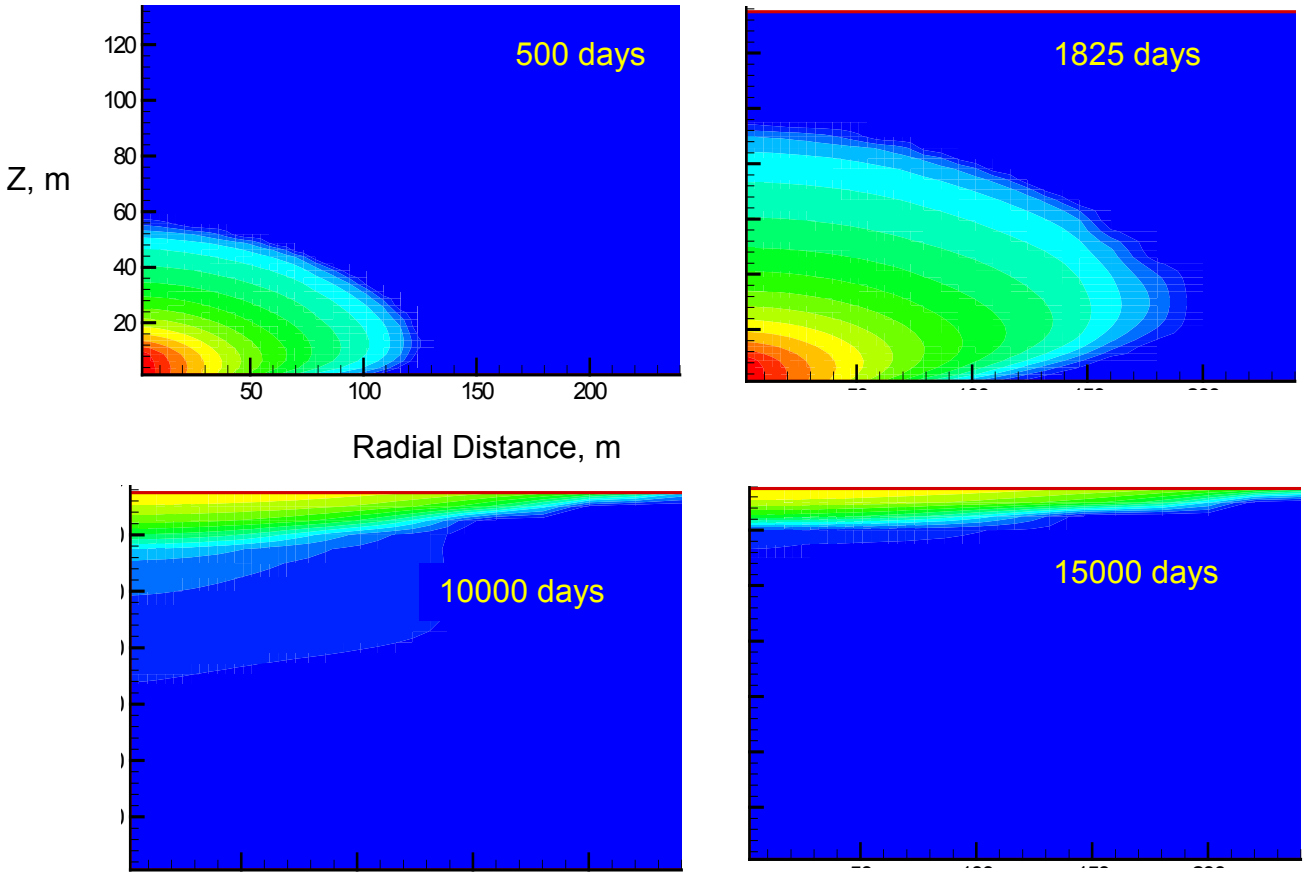


Fig. 5. Results from STOMP-CO2 simulation: CO2 bubble growth with time